Rheol Acta (2002) 41: 134–143

ORIGINAL CONTRIBUTION

Joachim Götz
Wolfgang Kreibich
Marian Peciar

Extrusion of pastes with a piston extruder for the determination of the local solid and fluid concentration, the local porosity and saturation and displacement profiles by means of NMR imaging

Received: 8 May 2000
Accepted: 1 May 2001

J. Götz (✉)
Institut für Mechanische Verfahrenstechnik und Mechanik
Universität Karlsruhe (TH)
Postfach 6380, 76131 Karlsruhe, Germany
e-mail: Joachim.Goetz@bl.tum.de

W. Kreibich
Bruker Medical Gmbh
Rudolf-Plank-Str.23
76275 Ettlingen, Germany

M. Peciar
Slovenska Technicka Univerzita
Bratislava, Slovac Republic

J. Götz
Present address: Lehrstuhl für Brauereianlagen und Lebensmittel-Verpackungstechnik, TU München
Weihenstephaner Steig 22
85350 Freising-Weihenstephan, Germany

Abstract Nuclear Magnetic Resonance (NMR) was used to investigate the extrusion behaviour of PTFE pastes in a ram extruder. By means of ^{1}H-NMR imaging (MRI) it is possible to determine the local proton density and therefore, the local fluid concentration. The ^{19}F-MRI provides the local solid concentration. Thus the local saturation and the local porosity can be calculated with the information of the local fluid and solid concentration. Furthermore displacement profiles can be derived from NMR images by means of correlation techniques without any preparation or marking of the pastes.

Key words Pastes · Extrusion · Piston extruder · Local porosity and saturation · Fluid and solid concentration · Displacement profiles

Introduction

In process engineering, the handling and extrusion of highly concentrated disperse systems play an important role. Examples are filtered colour pigments, pharmaceutical products, slurries, pumped concrete, ceramics and foods. Should the disperse phase consist of solid particles and possess a saturation approaching 100%, then the liquid phase approximately fills the void between the particles in contact with each other. As a result, the rheological behaviour of such pastes is a combination of that of a bulk material and a suspension. Some fundamental research has been conducted into the basic mechanics, especially when more than simple shearing is involved (e.g. Bird et al. 1983; Buggisch and Stadler 1986; Raschka 1990; Felder 1990; Roco 1992; Gleißle et al. 1993; Götz et al. 1993, 1994; Götz 1994; Buggisch 1995; Britton and Callaghan 1997). Hence, it is desirable to acquire sufficient empirical knowledge concerning the rheology of extrusion processes upon which theoretical models can be based, with non-invasive and contact-free experimental techniques that do not interfere with the deformation.

Hayashi et al. (1988) used MRI to observe advanced ceramics during the slip casting process. Altobelli et al. (1997) studied the fluid concentration and the velocity profiles of model suspensions undergoing extrusion, Rauwendaal (1990) extrusion of filled polymers and Sinton et al. (1990) the mixing of different filled polymers (saturated suspensions) in a twin-screw extruder. McCarthy et al. (1992), McCarthy and McCarthy (1994) and Seymour et al. (1995) applied MRI to

studying the velocity profiles during the extrusion processing of a simple, one-phase model fluid (carboxymethyl cellulose solution) and Rombach et al. (1998) studied the flow of water through a model extruder.

In contrast to the papers described above, real three-phase pasty suspensions were studied in this contribution which focuses on demonstrating the particular possibilities which NMR techniques offer with respect to the recording and characterisation of the extrusion processes of pastes. With two independent MRI techniques, ^{1}H- and ^{19}F-MRI, the local fluid, gas and solid concentration of pastes can be determined. MRI should yield a more comprehensive insight into the coupled phenomena of the structural changes and internal flow of pasty systems subjected to a deformation: cracks or shear planes, hollows, inner agglomeration processes and internal flow of free water relatively to the solid matrix (solid plus adsorbed, immobilised water) (Götz et al. 1993).

Materials

In this study only pastes of commercial PTFE powder (Hostaflon TF1750, Hoechst 1990) as solid and distilled water were used. PTFE pastes are, in many respects, characteristic of industrially relevant materials and are themselves used for extrudates and coatings. Hostaflon is a very fine-grained, non-free-flowing, high-molecular weight PTFE powder produced in a suspension polymerisation. The mean particle size is $d_{50} = 0.45\ \mu$m, the bulk density is 370 kg/m^3 and the density of sintered PTFE powder is 2160 kg/m^3 (Hoechst 1990). PTFE pastes were selected for the experiments because the solid contains fluorine, but no hydrogen, and the fluid contains hydrogen, but no fluorine (see below). The second reason was that they can be regarded as a model system for some pastes. The experimental results presented in this work show that the PTFE water pastes show an extrusion and crack behaviour similar to pastes with Pural (Condea GmbH, Hamburg) as solid. Pural is an oxide ceramic used for catalysts or catalysts carriers (Götz et al. 1993). Limestone pastes on the other hand show a totally different extrusion behaviour (Felder 1990; Götz 1994). Even this little selection of pastes shows that there is not a single model paste which can be used for all pastes because the flow behaviour of pastes is so complex and manifold. PTFE pastes were chosen for the experiments presented in this paper because they are used in industrial extrusion processes, as they have a flow behaviour similar to Pural pastes and also some specific magnetic qualities.

Standard washing-up liquid was added as detergent to the water (2.5 vol.%) in order to reduce the surface tension. The PTFE water pastes were mixed using a common household mixer. As both components are weighed individually and then subsequently mixed, the moisture content is most conveniently defined as

$$F = \frac{m_{liquid}}{m_{solid} + m_{liquid}} \tag{1}$$

where m_{liquid} is the mass of the liquid and m_{solid} of the solid.

In the following passage some fundamental definitions for the characterisation of pastes are given. The whole volume V of a moist bulk material can be divided into solid volume V_S, the fluid volume V_L and the gas volume V_G. The volume filled with water and gas $V_H = V_L + V_G$ is called pore volume. The volumetric ratios are:

– Solid volume concentration c_S (determined with ^{19}F-NMR)

$$c_S = \frac{V_S}{V} \tag{2}$$

– Fluid volume concentration (fluid fraction) c_F (determined with ^{1}H-NMR)

$$c_F = \frac{V_L}{V} \tag{3}$$

– Porosity ε (derived from c_S and c_F)

$$\varepsilon = \frac{V_H}{V} = 1 - c_S \tag{4}$$

– Saturation S (derived from c_S and c_F)

$$S = \frac{V_L}{V_H} = \frac{V_L}{V}\frac{V}{V_H} = c_F\frac{1}{\varepsilon} = \frac{c_F}{1 - c_S} \tag{5}$$

Nuclear magnetic resonance

NMR (Bloch et al. 1946; Purcell et al. 1946; Callaghan 1991; Kimmich 1997) stems from the fact that the nuclei of specific isotopes (e.g. of the hydrogen isotope ^{1}H and ^{19}F) possess a magnetic moment (spin) and are precessing under a specific angle with respect to an external magnetic field:

$$\mathbf{B}_O = B_O\ (0, 0, 1) \tag{6}$$

In the case of spin $^1/_2$ nuclei their components along the field axis ($\mathbf{B}_o$) are either parallel or anti-parallel to $\mathbf{B}_o$. Because the parallel orientation is for ^{1}H energetically preferable, this orientation is assumed by a larger number of nuclear spins.

Despite the fact that this phenomenon can be calculated correctly in physically terms only through use of quantum mechanics (e.g. Abragam 1961), the macroscopic behaviour of the spin ensembles can be described for many of the NMR experiments as a continuous magnetisation vector. In this description, the magnetisation vector in the thermal equilibrium points in the direction of the static magnetic field of the magnet. As soon as an RF field is switched, the magnetisation vector assumes a component orthogonal to the steady field and begins to precess with the Larmor frequency which is proportional to the magnetic field strength:

$$\omega = \gamma B_O \tag{7}$$

where γ is the gyromagnetic ratio of the respective isotope. This NMR principle established a large number of applications in analytical chemistry known collectively as NMR spectroscopy due to the fact that the exact resonance frequency for each nucleus is dependent upon the chemical environment of this nucleus (Ernst et al.

1987). The resonance frequency of ^{1}H is 42.55 MHz and 40.05 MHz for ^{19}F at $B_o = 1$ Tesla. This means ^{1}H and ^{19}F can be distinguished by means of their resonance frequencies and therefore also materials containing ^{1}H or ^{19}F.

In order to determine the solid and fluid concentration it is theoretically also possible to use other NMR parameters such as T_1, T_2 or $T_{1\rho}$ to distinguish between the solid and the fluid components (e.g. T_2 in Götz et al. 1994). The disadvantage of these solutions is that the local concentration of the solid and the fluid cannot be measured directly, but must be derived by assuming the according relaxation behaviour.

In order to derive information concerning the spatial distribution of the spins, and hence of the moisture within the material, the homogeneous magnetic field $\mathbf{B}_o$ must have additional fields derived by defined gradients $\mathbf{G}_x$ (called read-gradient) superimposed on it during the excitation and the detection of the NMR signal. As a result, the NMR signal contains spatial information. The resonance frequency varies along the sample in accordance with

$$\omega(\mathbf{r}) = \gamma(\mathbf{B}_O + \mathbf{G}_x \times \mathbf{r}) \tag{8}$$

Another principle which provides spatial information is the use of a gradient $\mathbf{G}_y$ (called phase-gradient) between the excitation and detection. With this process, the signal phases are dependent upon the location in the direction of this second gradient. The excitation must be repeated with a linear variation of the strength of the phase gradient.

The standard imaging experiment consists of applying a read-gradient and then a phase-gradient orthogonal to the direction of the read-gradient. By repeating the experiment under variation of the phase-gradient, a two-dimensional matrix of signals is produced. The image is derived by Fourier transformation in each direction; for this reason, such experiments are entitled 2DFT (two dimensional Fourier transformation). The spatial restriction of the signal in the third direction is usually achieved through use of a slice selection gradient $\mathbf{G}_z$ during the excitation pulse, which produces a slice thickness of $\Delta z = \Delta\omega/\gamma G_z$.

Several imaging strategies have been developed for an effective determination of the spatial distribution of the hydrogen and fluorine density (Callaghan 1991; Blümich 2000). The sequences for the NMR tomography (MRI) used in this investigation are described below. In every MRI-experiment the sample is divided into a matrix of three-dimensional voxels. The size of each voxel is established by the field of view (FOV) selected, which relates to the dimensions of the measuring volume in the magnet as well as to the matrix size (number of voxels according to the relevant spatial dimensions).

Spin echo imaging

We used a Spin-Echo sequence (MSME) with variable echo time (Callaghan 1991). The parameters important for imaging were (typical values are provided in parentheses):

I	nucleus: ^{1}H
TE	echo time (= 4 ms)
TR	recovery time (= 4000 ms)
M	matrix size ($= 256 \times 256$)
AV	averages (= 1)
FOV	field of view (= 60 mm)
ST	slice thickness (= 1.5 mm)
a	resolution (a = FOV/M) (= 0.23 mm)

Single point imaging (SPI)

The imaging of materials with extremely short T_2-times has not been hitherto possible because the echo times are usually in the range of several milliseconds. The SPI-sequence enables detection times of a few microseconds (Nauerth and Gewiese 1993), which is significantly shorter than gradient-switching times. Thus the fluorine isotope ^{19}F in solid PTFE, whose relaxation time is shorter than 1 ms, can also be used for imaging. The disadvantage of the sequence is the long total scan time since every point in k-space must be measured successively and is not scanned in lines as in MSME. This experiment is also 2DFT in type, but also uses a phase-gradient in the first direction instead of a read-gradient. For producing spatial information, the experiment must be repeated with variation of the gradient strength; for this reason the experiment is considerably longer than a standard imaging experiment. In fact, this sequence requires a spatially encoding phase gradient in the third direction as well, since the use of a slice selection scheme would increase the time for the detection of the signal into the range of a millisecond.

Excitation and detection are performed under conditions of a constant gradient. For this reason, the detection time can be shorter than the gradient-switching time. Furthermore, many averages are necessary in order to obtain a sufficient signal-to-noise ratio. The parameters important for imaging were (typical values are provided in parentheses):

I	nucleus: ^{19}F
TD	detection time (“echo time”) (= 40 μs)
T_R	recovery time before the next pulse (= 2 ms)
M	matrix size in k-space→r-space (k: 45^3→R: 64^3)
AV	averages = 240
FOV	field of view (= 100 mm)
a	resolution (= 1.6 mm)

Combination of ^{1}H-MRI and ^{19}F-MRI

On a microscopic scale, pastes are a multi-phase system consisting of finely dispersed solid particles, a fluid (capable of forming drops) and eventually gas inclusions or hollows. Previously it has only been possible to determine the local fluid concentration. If the paste is a three-phase system of solid/fluid/gas, an unambiguous interpretation of the experimental data has not been possible up to now. An example of this would be the change of the moisture during the extrusion. If the paste is not completely saturated this could mean that the porosity and/or the saturation has increased. The same holds true for the fluid concentration. Examples of processes where separation, inner flow and local structural changes play a role have already been described (Götz 1994). The temporal change of the mean moisture of a paste during extrusion, as a consequence of inner flow in addition to the compressibility of the solid matrix (Felder 1990) and moisture distributions with differences greater than 30% in the volume (at one time) in a capillary (Götz 1994), make it particularly plausible that capillary rheometry is not appropriate to characterise the strong moisture-dependent flow behaviour of disperse systems which tend to separation. Thus results obtained cannot be transferred or are totally meaningless, since the prerequisites [defined velocity profiles, homogeneity (sedimentation, phase separation, preparation and time effects), continuum mechanics (scale effects), crushing (Weipert et al. 1993), wall slip and filling ratio of the rheometer] required to derive the material parameters are not fulfilled. In order to decide whether the porosity and/or the saturation is changing, it is necessary to know the local fluid and solid concentrations. For PTFE-pastes, solid and fluid components can be distinguished by means of their resonance frequencies.

The local resolution for the experimental set-up in the BIOSPEC is 100 μm for ^{1}H and 1 mm for ^{19}F. Extrusion experiments with PTFE-pastes can provide an important contribution to a better understanding of the flow behaviour and perhaps the crack behaviour of pastes. The information is limited only by the resolution presently achieved for ^{1}H- and ^{19}F-MRI.

For pastes, whose solid contains fluorine but no hydrogen (e.g. PTFE) and whose fluid contains hydrogen but no fluorine (e.g. water), the local fluid (c_F) and solid concentration (c_S) can be determined independently. Thus the local saturation and porosity can be derived (see above).

Magnet

The extrusion experiments were conducted in an NMR tomograph BIOSPEC 24/40 (BRUKER MEDICAL GMBH, Ettlingen) with a 40-cm bore, a B_o field of 2.35 Tesla and thus a ^{1}H-frequency of 100 MHz as well as a ^{19}F frequency of 94 MHz. The gradients are generated on a high performance actively shielded streamline mini-imaging insert with an inner diameter of 120 mm and a maximum gradient strength of 188 mT/m (100 A). The gradient rise time was 250 μs. The RF coil employed was double tuned to ^{1}H and ^{19}F with an inner diameter of 72 mm. The entire probehead was constructed in such a way that it did not provide any ^{19}F background signal. This is not easy, since some commercial coaxial cables contain PFTE as dielectric.

Experimental results

The extrusion experiments were conducted in a piston extruder constructed entirely of PVC (Fig. 1). PVC does not contribute to the ^{1}H signal (MSME) for the parameters specified earlier. The cylinder is 400 mm long with an interior diameter of 40 mm. We used two dies: a one-hole die with an interior diameter of 23.3 mm and a relative free area of 34% (Fig. 2a) and a multi-hole die with a relative free area of 25% (Fig. 2b). The aim of the experiments was to study the influence of the geometry in simple dies which are used for industrial extrusion.

Extrusion experiments

The piston extruder was filled and installed into the magnet. For a given piston displacement a 2-D or a 3-D

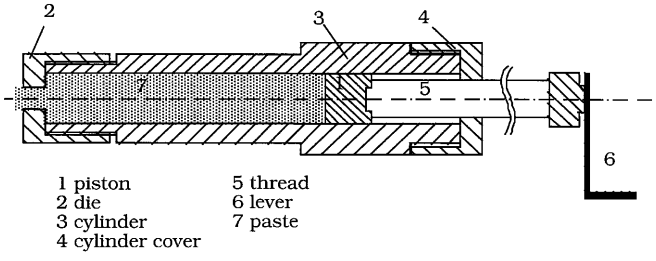

Fig. 1 Schematic of the piston extruder

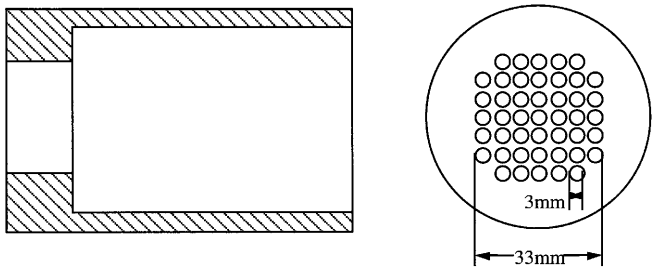

Fig. 2 Dies: *left* – single-hole die (sectional plane: axial); *right* – multi-hole die (sectional plane: radial)

image was taken. Afterwards the piston was displaced for a certain distance and the MRI-experiment was repeated. The longitudinal or transversal sections through the tube axis for extrusion experiments with a one-hole and multi-hole die thus obtained were recorded. The intensity of the signal is proportional to the local fluid concentration (^{1}H) and the local solid concentration (^{19}F), respectively. In ^{1}H-MRI dark stands for no fluid and the brighter the intensity, the higher the fluid concentration. That means the brighter the pixel, the higher the volume concentration of ^{1}H and ^{19}F, respectively. In order to obtain absolute concentrations, a water-filled tube (^{1}H) and a PTFE stick (^{19}F) was fixed at the front side of the dies, above and below the mouth. The water filled tube can be seen in the ^{1}H-image as a light circle ($c_F = 100\%$), PTFE stick in the ^{1}H-image as dark circle and in the ^{19}F-image as a bright circle ($c_S = 100\%$). High ^{1}H-intensity correlates with high local moisture.

One-hole die. Two moistures $F = 35$ and 41% were investigated. Figures 3 and 4 show a series of longitudinal sections (containing the pipe axis) of the filled piston extruder. The displacement increases from left to right and from the top down. In Fig. 5 control volumes are defined. The fluid concentration c_F (Fig. 6) in the inside of the piston extruder decreases for both moistures with increasing displacement of the piston. This provides an indication of internal flow of water relatively to the solid matrix (Fig. 6). On the other hand, c_F in the extrudate, to be more precise in the die, increases to a certain extent. At the beginning of the extrusion water is obviously pressed out, flows out of the die and surrounds the cylinder of PTFE (dark in the ^{1}H-images). For the lower $F = 35\%$ plug flow can be supposed (Fig. 4). This can be verified by results obtained through a combination of MRI and Digital Speckle Photography and presented subsequently. Graczyk et al. (1990) showed with the help of coloured marks that these pastes that are suitable for extrusion show plug-flow within the die.

The mean value of c_F in the extrudate is significantly higher than in the cylinder interior. For $F = 41\%$ c_F in the cylinder interior decreases from 33% to 26%, in the extrudate c_F is about 47%, the piston displacement

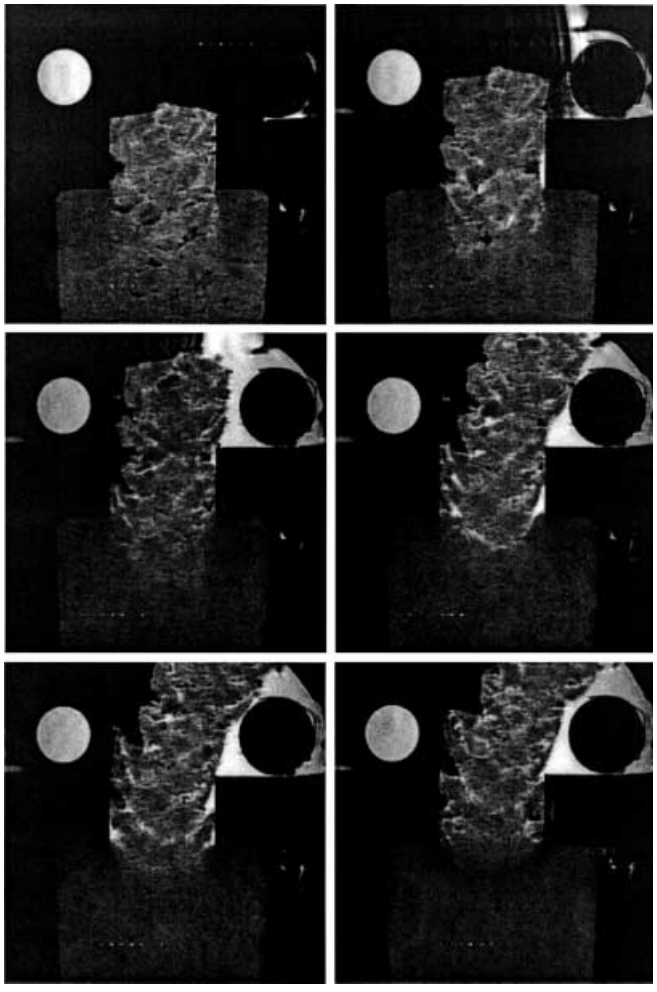

Fig. 3a–f Extrusion of a paste with $F = 41\%$. The signal is the local fluid concentration (^{1}H-density). Piston displacement: **a** 14; **b** 22; **c** 30; **d** 38; **e** 46; **f** 54 mm. $TE = 8.7$ ms, $T_R = 400$ ms, $FOV = 60$ mm, $M = 256 \times 256$, $a = 0.23$ mm, $ST = 1.5$ mm

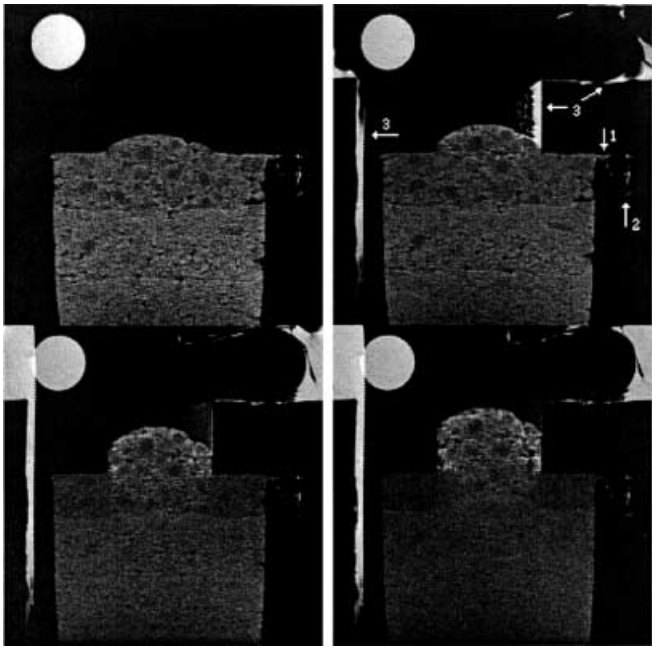

Fig. 4a–d Extrusion of a paste with $F = 35\%$. The signal is the local fluid concentration (^{1}H-density). Mark 1 is due to the incompletely screwed-on die, mark 2 due to water in the thread between the die and the piston extruder and mark 3 due to the pressed-out water. Piston displacement: **a** 0; **b** 9; **c** 20; **d** 30 mm. $TE = 10$ ms, $T_R = 300$ ms, $FOV = 60$ mm, $M = 512 \times 512$, $a = 0.11$ mm, $ST = 1.5$ mm

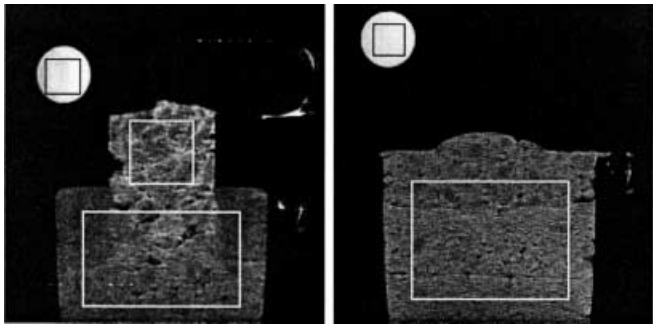

Fig. 5 Control volumes for the determination of the fluid concentration during the extrusion process: *left* – Fig. 3; *right* – Fig. 4

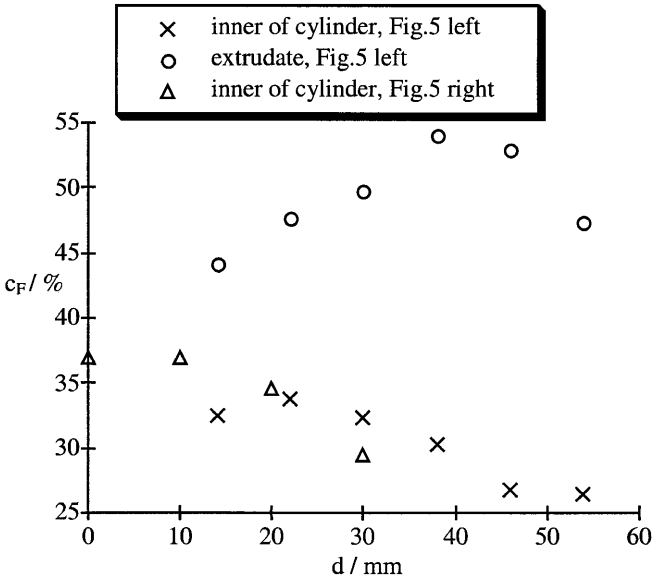

Fig. 6 Fluid concentration c_F in control volumes (Fig. 5) as a function of the piston displacement d

40 mm (Fig. 3a–f). For F = 35% c_F in the cylinder interior decreases from 37% to 28% after a piston displacement of 30 mm (Fig. 4a–d). Dry regions form at the piston and in the dead zones below the closed areas of the die. This is obviously the cause of the simultaneous increase in pressure. While the material is compressed in the piston extruder, hollows appear in front of the die which are partly air-filled (dark), partly water-filled (bright). This can be clearly seen in the upper images of Fig. 3. These hollows might be one of the reasons for cracks which can be detected in the extrudates (Fig. 3, lower images). These cracks are known as "shark skin" and appear also in Pural pastes (Götz et al. 1993). The existence of theses cracks is a significant problem, since such extrudates are worthless.

Multi-hole die. Only a small part of the paste can be extruded for F = 41% in a multi-hole die (Fig. 7); the biggest part of the extruded material is pure water. The

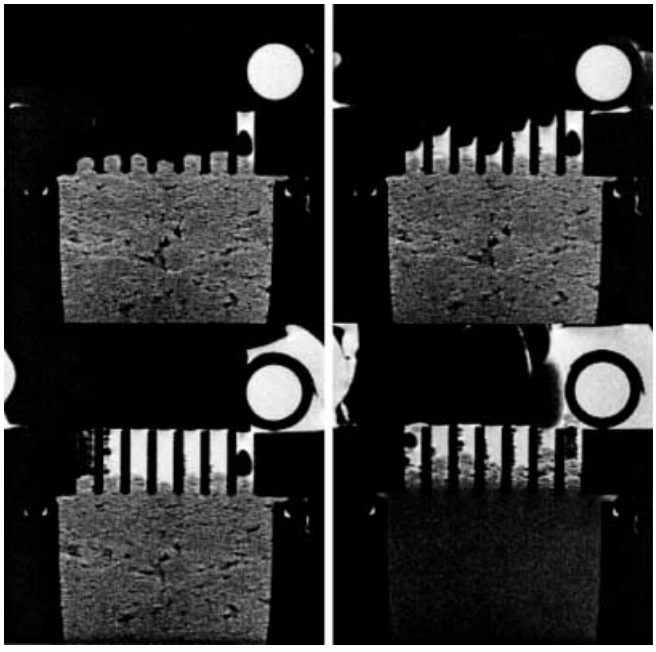

Fig. 7 Extrusion of a paste with F = 41% in a multi-hole die. The signal is the local fluid concentration (^{1}H-density). Piston displacement: 0, 4, 10, 26 mm. TE = 10 ms, T_R = 600 ms, FOV = 60 mm, M = 256 × 256, a = 0.23 mm, ST = 1.5 mm

average fluid concentration decreases from initially c_F = 36% (after a piston displacement of 26 mm) to 24%. The significant decrease of the hollows makes one conclude that the solid matrix was compressed.

From the extrusion of pastes it is a known phenomenon that the moisture of the extruded material F increases during the extrusion process (Felder 1990). The extent of the dewatering depends for example on the powder (material, particle size distribution), the initial moisture and of course on the extruder and die material and the die geometry. The used multi-hole die causes more of a filtration of the PTFE paste than an extrusion. This is due to the flow behaviour of the PTFE paste and not to the design of the piston extruder as extrusion experiments with limestone pastes and Pural pastes prove (Götz et al. 1993).

Evaluation

^{19}F-MRI was not possible for all piston positions because of the long total imaging time (about 11 h). Therefore, the measured ^{1}H-(fluid-) (Fig. 8a, F = 35%) and ^{19}F-(solid-)images (Fig. 8b) and the porosity (Fig. 8c) and saturation (Fig. 8d) distributions derived from these (see above) are only presented for special experiments. The significant decrease of the solid concentration in the extrudate, the increase of the solid concentration at the walls and the shark skin are

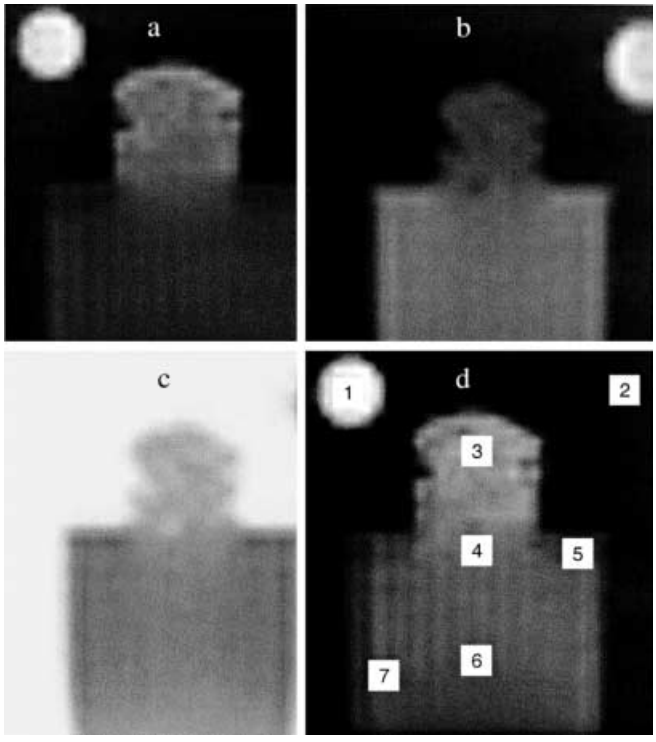

Fig. 8 a ^{1}H-density (fluid concentration) of a paste after a piston displacement of 50 mm. The lower resolution (in comparison with Fig. 4) is due to using the same parameters as in the ^{19}F-images. F = 35%, Sequence: MSME, TE = 4 ms, T_R = 1500 ms, FOV = 100 mm, M = 64 × 64, a = 1.5 mm, ST = 2 mm. **b** ^{19}F-density (solid concentration) c_S of PTFE-water paste. The resolution is 1.5 mm, the total imaging time 11 h. Low signal intensity results from low solid concentration and high signal intensity results from high solid concentration. Sequence: SPI, TD = 40 μs, T_R = 2 ms. **c** Local porosity. **d** Local saturation. The numbers mark the positions in Table 1

remarkable (Fig. 8a). The intensity in Fig. 8c,d is proportional to the values of the porosity and the saturation. In Table 1 local fluid and solid concentrations, the local porosity and the local saturation are shown at selected positions (in volume percentage = vol.%).

In Table 1 the significant increase of the porosity in the extruded material is remarkable. This could cause a low undesirable mechanical stability of the extrudates. High porosities are only intended and necessary for the functionality of extrudates which are used for catalysts or catalyst barriers. On the other hand, the porosity in the dead zones (5), near the walls (7) and towards the piston (6) decreased. This is a consequence of the compressibility of the solid matrix (solid plus immobilised fluid, not the solid particle itself). Two things are remarkable with regard to the saturation. First is the increase of the saturation in the extrudate. Water flows into existing hollows (c_F increases). The solid matrix is compacted in the piston interior (c_S increases, ε decreases) (Eq. 5). Second, there is a decrease of the saturation in the whole interior of the extruder due to the pressing out of water.

These phenomena can also be observed for F = 41% (Fig. 9). The extrusion through the multi-hole die shows that c_F, c_S, ε and S almost only vary in the axial direction (that means from below to above in the single images) (Fig. 10). The radial dependency is negligible. This could be expected because of the plug flow of the paste in the interior (apart from the entrance of the die) of the extruder. c_F is at the piston and at the die smaller than in

Table 1 Fluid and solid concentration, local porosity and saturation in vol.% (Fig. 8). The accuracy is about 1 vol.%

	Position (Fig. 9d)	c_F	c_S	ε	S
1	Calibration sample (water)	100	0	100	100
2	Calibration sample (PTFE)	0	100	0	0
3	End of the extrudate	46	28	71	66
4	Beginning of the extrudate	31	38	62	52
5	Dead zone	15	50	50	36
6	Interior of the extruder/middle	20	43	57	36
7	Interior of the extruder/outside	18	45	55	34

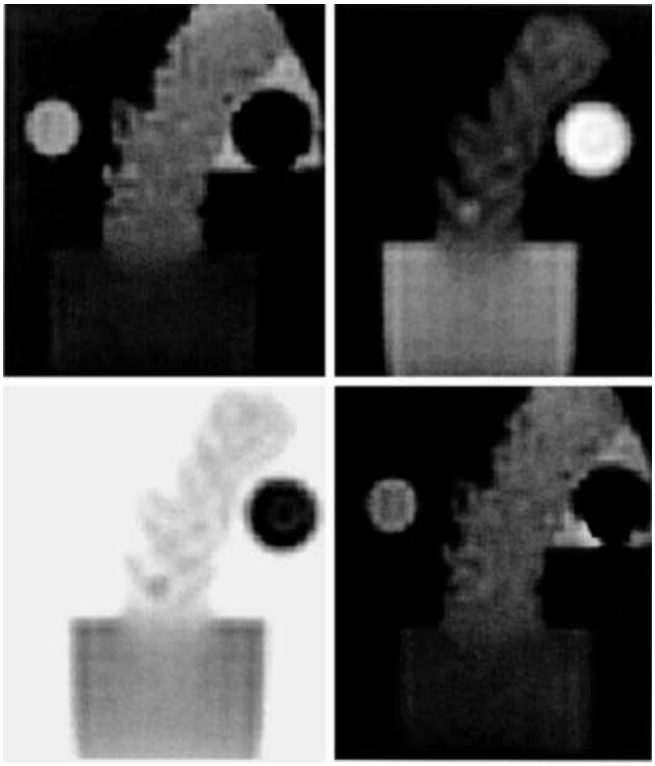

Fig. 9a–d Extrusion of a paste with F = 41% in a single-hole die. Fluid concentration (*left above*), solid concentration (*right above*), local porosity (*left below*) and local saturation (*right below*). Piston displacement: 54 mm both: FOV = 100 mm, M = 64 × 64, a = 1.5 mm, ST = 2 mm. ^{1}H-MRI (*left above*): TE = 4 ms, T_R = 6000 ms. ^{19}F-MRI (*right above*): TD = 40 μs, T_R = 2 ms

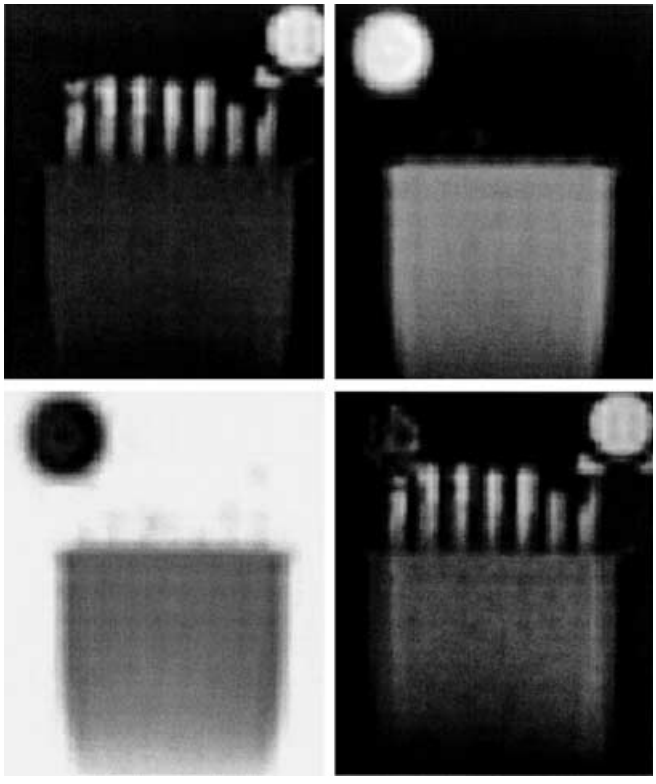

Fig. 10 Extrusion of a paste with F = 41% in a multi-hole die. Fluid concentration (*left above*), solid concentration (*right above*), local porosity (*left below*) and local saturation (*right below*). Piston displacement: 108 mm. both: FOV = 100 mm, M = 64 × 64, a = 1.5 mm, ST = 2 mm. ^{1}H-MRI (*left above*): TE = 5 ms, T_R = 900 ms. ^{19}F-MRI (*right above*): TD = 40 μs, T_R = 2 ms

the interior. c_S decreases continuously from the piston to the die. Comparatively little solid is extruded and an over-proportional ratio of water is pressed out. ε and S decrease due to internal flow of water. S is higher in the extrudate because mainly water is pressed out. The present results show that a combination of ^{1}H-MRI and ^{19}F-MRI enables an unambiguous local characterisation of pasty and multi-phase systems.

Displacement profiles

In PTFE pastes, the cavities or gas inclusions do not disappear, even after large deformations. With such substances one can obtain the local displacement of the paste without marking or imprinting any structures during the extrusion process. This technique based on the Digital Speckle Correlation (DSC) has been developed for the determination of the displacement field at the surface of foams (Wolf 1996; Wolf et al. 1996). In the present study this technique was applied to MRI images of pastes. Two successive ^{1}H-images (Fig. 11a)

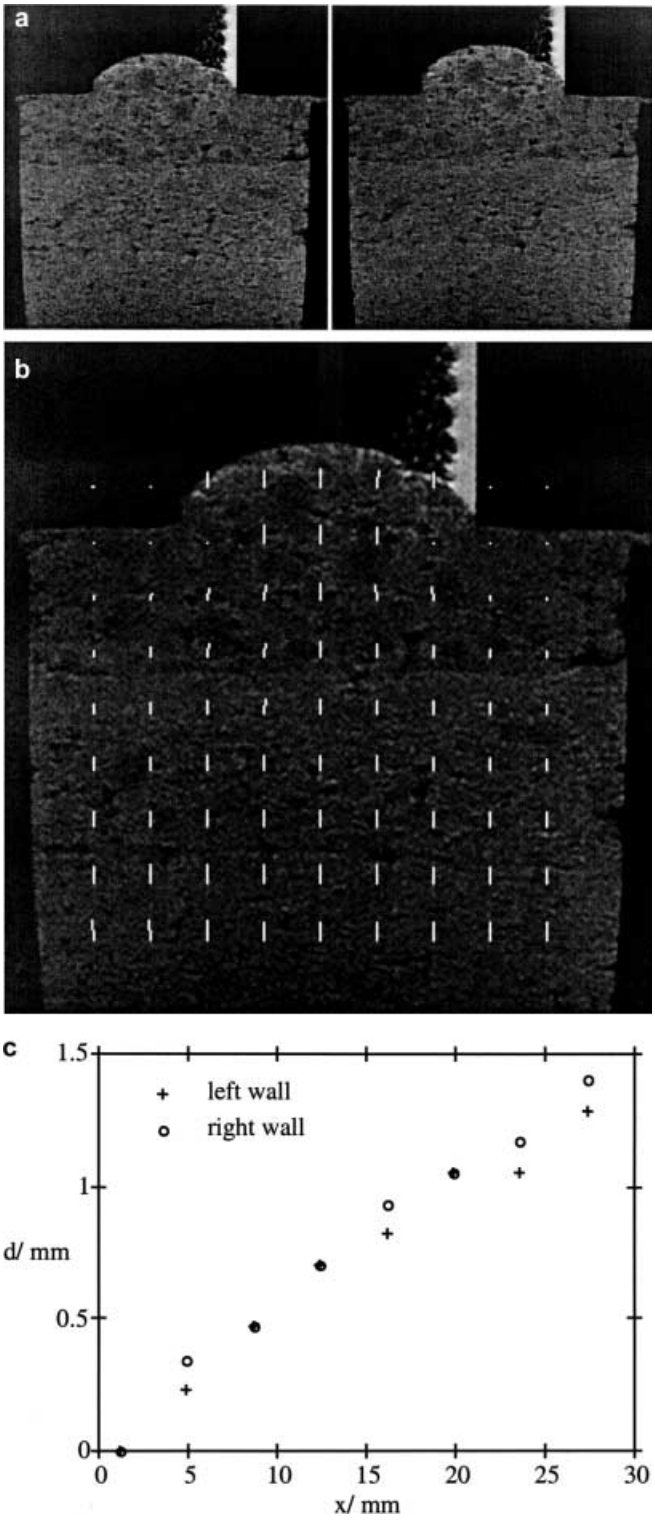

Fig. 11 a Extrusion of a paste with F = 35% in a single-hole die. Piston displacement: 8 mm (*left*), 12 mm (*right*). **b** Displacement field, M = 512 × 512, submatrix: 64 × 64. **c** Absolute value d of the displacement vectors near the walls of the piston extruder as a function x (distance from the die) according to Fig. 11a

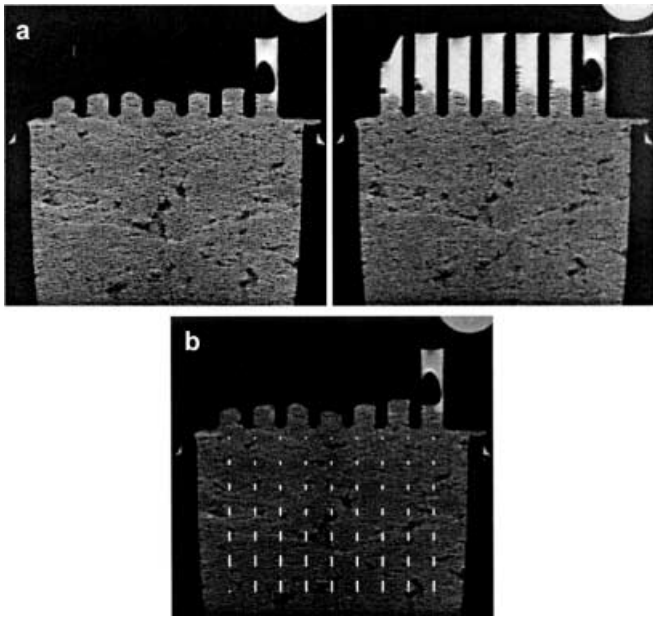

Fig. 12 **a** Extrusion of a paste with F = 41% in a multi-hole die. Piston displacement: 0 mm (*left*), 8 mm (*right*). **b** Displacement field, M = 256 × 256, submatrix: 32 × 3

were cross-correlated after the matrix has been divided into submatrices (each submatrix consists of several voxels). The position of the maximum of the correlation function marks the mean local displacement of the corresponding submatrix (Fig. 11b). The absolute value of the displacement vectors decrease for a paste (F = 35%) in a single-hole die in the direction of the piston-movement. Only near the die can a large increase of the magnitude of the displacement vectors be observed (Fig. 11c).

In a multi-hole die the displacements decrease almost linearly towards the die in a plug-flow (Fig. 12). The solid matrix is more and more compacted during the extrusion. The compressibility of the solid matrix can be attributed to the fact that (a) the water is partly pressed out and (b) pastes are generally not entirely saturated, but a three-phase system consisting of solid, fluid and gas. For large piston displacements the vector field calculated with cross-correlation is physically not correct. No sufficient structures can be detected within the paste after the compression of the solid matrix.

Conclusions

Extrusion experiments were performed with PTFE-pastes using two moistures and two dies. The extrusion was selected as an example of an industrially relevant process, PTFE-water paste as a material with model character and because it is used in the same consistency in industrial processes (e.g. coating) with similar moistures. With the help of two *independent* experiments, the local fluid concentration (^{1}H-MRI), the local solid concentration (^{19}F-MRI) and corresponding voids (gas) can be determined. As pastes are generally three-phase systems, the local saturation and porosity can be derived. Thus extrusion experiments can be characterised by means of MRI, locally, non-invasively and contact-free.

The extrudates have a solid concentration (28 vol.%) that is only half of the original filling (44%) of the extruder. The fluid concentration of the extrudate is 46% in comparison with 19% of the filling, which is due to an internal flow of part of the water relatively to the solid matrix. This corresponds to the fact that the porosity of the extrudate increased from 56 to 71% and the saturation even from 35 to 66%. This means that hollows arise in the material during the extrusion whose filling ratio is higher than in the original filling. If the internal flow exceeds the flow of the solid matrix too much, the process changes from an extrusion to a filtration. This depends on the paste, the extruder material and the geometry of the die. The hollows in the extrudate are big enough to be visible in the MRI images. Besides hollows, which are filled with gas and/or water, in the interior of the extrudates, shark skin (partly a third of the die diameter) also appears at the surface of the extrudate. These cracks arise in the die and seem to be caused by hollows arising in front of the die, in the extruder.

In order to study the processes during the press filtration of a paste (e.g. suspension of colour pigments or sewage sludge) the same device (Figs. 1 and 2) with a filter instead of a die could be used. Then it would for example be possible to correlate the local saturation in dewatered material with the stability or tensile strength of the filter cake. Korger (1995) showed that the solid-liquid separation caused by vapour-pressure dewatering can be monitored with MRI.

Displacement profiles can be derived from NMR images by means of correlation techniques (e.g. DSC) without any preparation or marking of the pastes. Prerequisite is that (a) sufficiently inhomogeneous structures are in the paste and that (b) not too big displacements exist between two images. This techniques fails at the end of the extrusion process after the material has been compacted. Furthermore the zones in consideration could be pushed out of the measuring volume.

Acknowledgements We would like to thank the DFG, Bonn, (project BU485/16) and the Fonds der Chemischen Industrie (Verband der Chemischen Industrie e.V., Frankfurt/Main) for financial support and Bruker Medical Gmbh, Ettlingen, for the technical and scientific support.

References

Abragam A (1961) Principles of nuclear magnetism. Clarendon Press, Oxford

Altobelli SA, Fukushima E, Mondy LA (1997) Nuclear magnetic resonance imaging of particle migration in suspensions undergoing extrusion. J Rheol 41(5):1105–1115

Bird RB, Dai GC, Yarusso BJ (1983) The rheology of viscoplastic materials. Rev Chem Eng 1(1)

Bloch F, Hansen WW, Packard M (1946) The nuclear induction experiment. Phys Rev 70:474–485

Blümich B (2000) NMR imaging of materials. Clarendon Press, Oxford

Britton MM, Callaghan PT (1997) NMR microscopy and the non-linear rheology of food materials. Magn Reson Chem 35:37–47

Buggisch H (1995) Über das zeitabhängige Fließverhalten von Pasten, CIT, 67, S. 1148, 1995

Buggisch H, Stadler R (1986) Shear flow of wet bulk solids. Proc der PARTEC Nürnberg

Callaghan PT (1991) Principles of nuclear magnetic resonance microscopy. Clarendon Press, Oxford

Ernst RR, Bodenhausen G, Wokaun A (1987) Principles of nuclear magnetic resonance in one and two dimensions. Clarendon Press, Oxford

Felder R (1990) Charakterisierung von Pasten mit einem Schergerät in Hinblick auf ihre Ausformbarkeit. Dissertation, Universität Karlsruhe

Gleißle W, Graczyk J, Buggisch H (1993) Rheological investigation of suspensions and ceramic pastes. KONA 11:125–137

Götz J (1994) Möglichkeiten der Kernspintomographie zur Diagnose von Strömungsvorgängen und Strukturänderungen in Pasten. Dissertation, Universität Karlsruhe

Götz J, Buggisch H, Peciar M (1993); NMR-imaging of pastes in a ram extruder. J Non-Newtonian Fluid Mech 49

Götz J, Müller D, Buggisch H, Tasche-Lara C (1994) NMR flow imaging of pastes in steady-state flows. Chem Eng Process 33

Graczyk J, Roth A, Gleißle W, Kotter M (1990) Fließeigenschaften von Keramiken für die Herstellung von Katalysatorträger. Erdöl Kohle Erdgas Petrochem Hydrocarbon Technol 43:27–30

Hayashi K, Kawashima K, Kose K, Inouye T (1988) NMR imaging of advanced ceramics during the slip casting process. J Phys D 21:1037–1039

Hoechst AG (1990) Product information Hostaflon TF 1750

Kimmich R (1997) NMR tomography diffusometry relaxometry. Springer, Berlin Heidelberg New York

Korger V (1995) Dampfdruckentwässerung – Ein neues kombiniertes Entfeuchtungsverfahren. Dissertation, Universität Karlsruhe

McCarthy MJ, McCarthy KL (1994) Sci Food Agric 65:257–261

McCarthy KL, Kauten RJ, Agemura CK (1992) Application of NMR imaging to the study of velocity profiles during extrusion processing. Trends Food Sci Technol. Aug/Sept(3)

Nauerth A, Gewiese B (1993) SMRM Book of Abstracts, 12th Meeting, p 1215

Purcell M, Torrey HC, Pound RV (1946) Resonance absorption by nuclear magnetic moments in a solid. Phys Rev 69:37

Raschka R (1990) Bestimmung der Fließeigenschaften feuchter Schüttgüter mit Anwendung bei der Schneckenextrusion, Dissertation, Universität Karlsruhe

Rauwendaal C (1990) Polymer extrusion. Hanser, München

Roco G (1992) Particulate two-phase flow. Butterworth-Heinemann, Boston

Rombach K, Laukemper-Ostendorf S, Blümler P (1998) Applications of NMR flow imaging in materials science. In: Blümler P, Blümich B, Botto R, Fukushima E (eds) Spatially resolved magnetic resonance. Methods, materials; medicine; biology; rheology; geology; ecology; hardware. Wiley-VCH, Weinheim

Seymour JD, Maneval JE, McCarthy KL, Powell RL, McCarthy MJ (1995) Rheological characterization of fluids using NMR velocity spectrum measurements. J Texture Stud 26(1):89–101

Sinton SW, Crowley JC, Lo GA, Kalyon DM, Jacob C (1990) Nuclear magnetic resonance imaging studies of mixing in a twin-screw extruder. ANTEC '90, pp 116–119

Weipert D, Tscheuschner H-D, Windhab E (1993) Rheologie der Lebensmittel. Behrs-Verlag, Hamburg

Wolf T (1996) Entwicklung eines optischen 3D-Verformungsanalyseverfahrens für geschäumte Polymere. Dissertation, Universität Karlsruhe

Wolf T, Gutmann B, Weber H, Ferré-Borrull J, Bosch S, Vallmitjana S (1996) Application of fuzzy-rule based postprocessing to correlation methods in pattern recognition. Appl Opt35:6955–6963